

ARTICLE

Electronic Supplementary Information:

Received 00th January 20xx,
Accepted 00th January 20xx

DOI: 10.1039/x0xx00000x

**Quasi-Low-Dimensional Perovskite with Enhanced Stability
Against Lattice Strain and Desired Band-Edge by A-Site Design**

Qi Liu and Xiao Cheng Zeng^{*a}

a Department of Material Science and Engineering, City University of Hong Kong,
Hong Kong SAR 999077, China. *Email: xzeng26@cityu.edu.hk

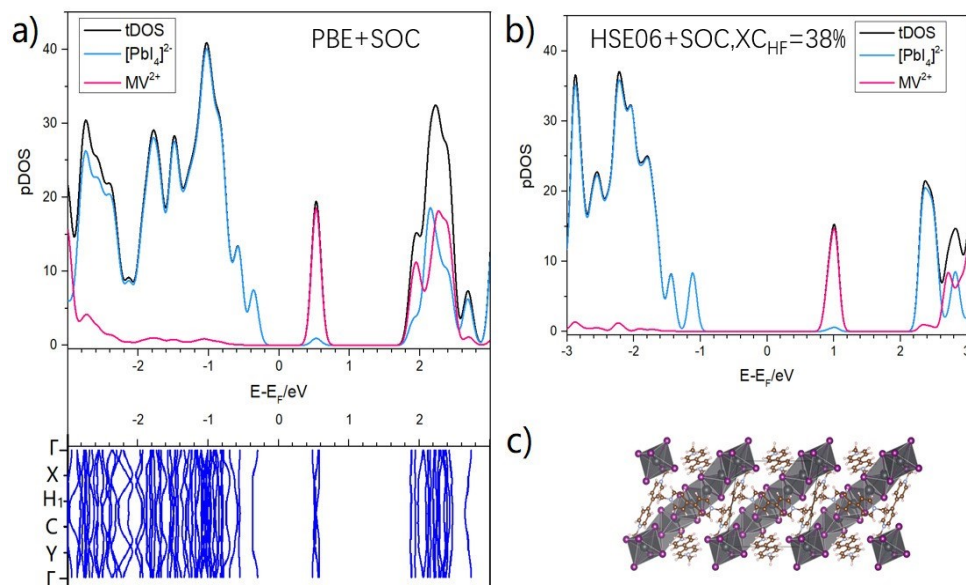


Figure S1: Computed (a) projected density-of-states and band structure at PBE+SOC level of theory, and (b) projected density-of-states at HSE06+SOC level of theory with an XC_{HF} fraction being 0.38 of the (c) structure of MV(PbI₃)₂ according to *Nature Communications* (2024) **15** : 2753.

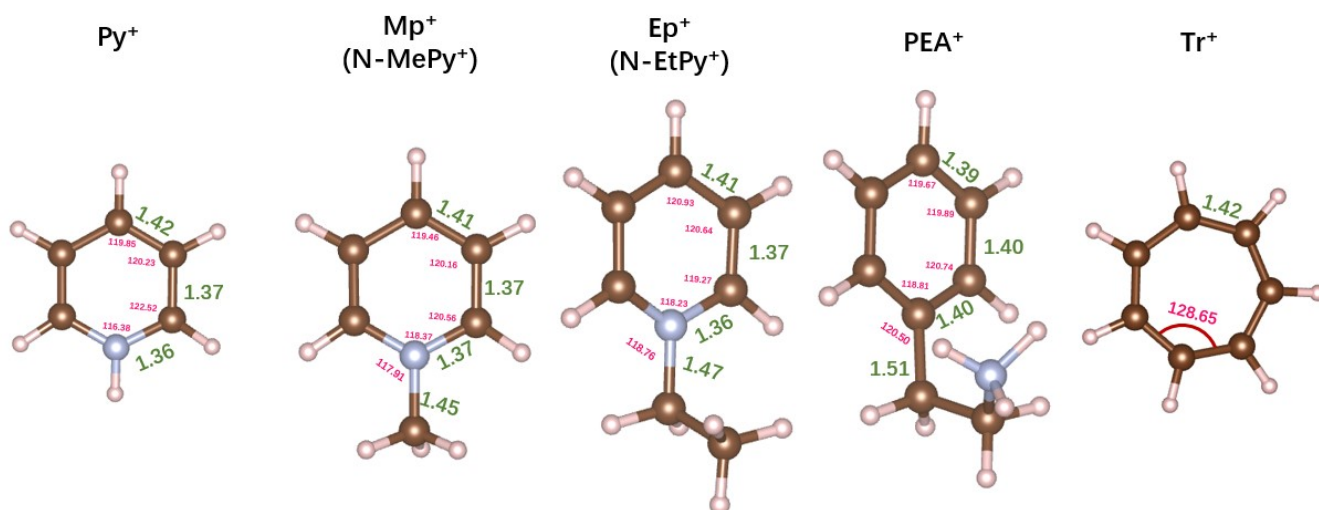


Figure S2: Optimized geometric parameters of the spacer cations adopted in this research. All the spacers are optimized as its iodide salt.

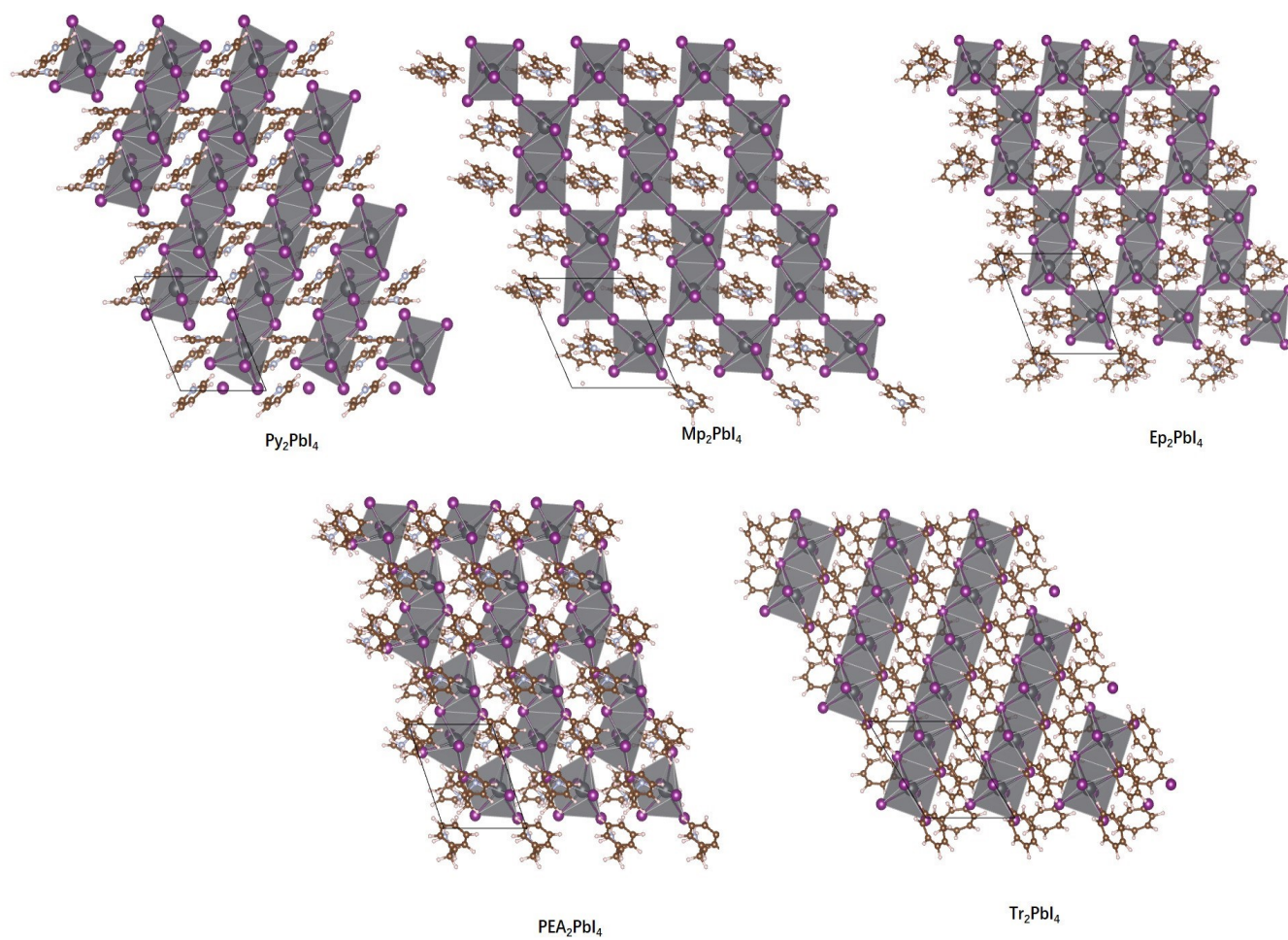


Figure S3: Top view of optimized CPAC-based QLD perovskite A₂PbI₄ supercells with various spacers.

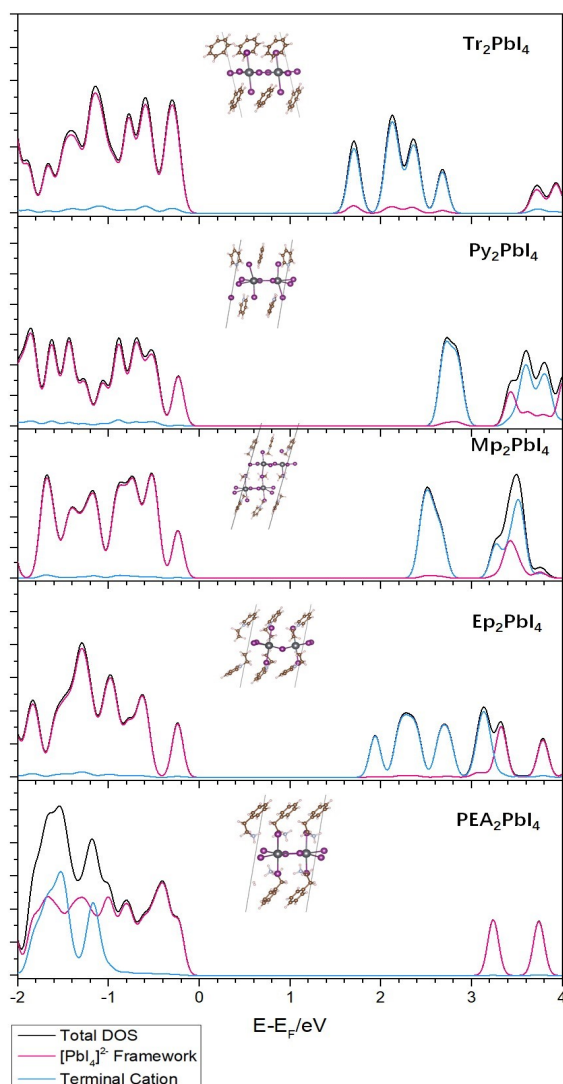


Figure S4: Computed projected density-of-states of rigid QLD A_2PbI_4 $A = Py, Mp, Ep, Tr,$ and PEA for benchmark at HSE06+SOC level of theory with an XC_{HF} fraction being 0.38.

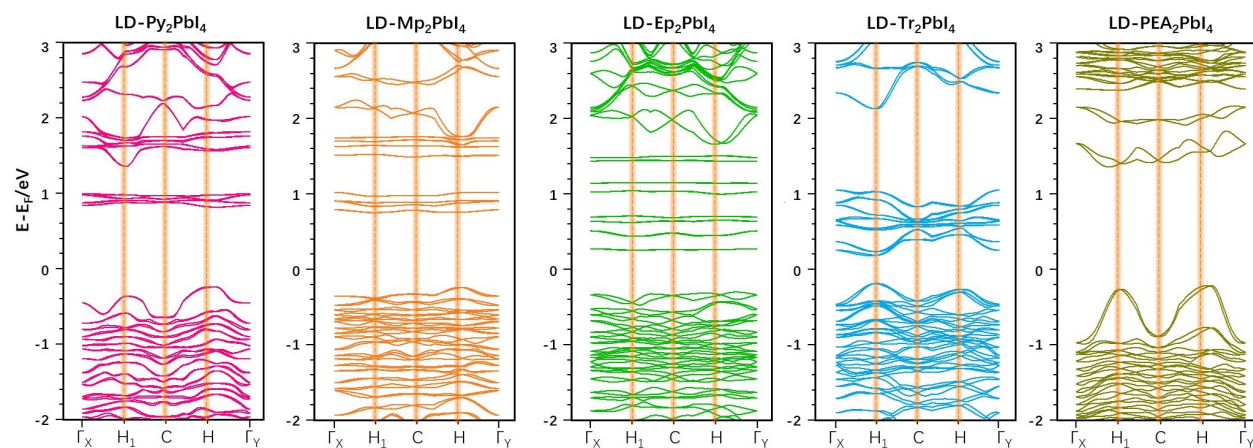


Figure S5: Computed band structure of rigid QLD A_2PbI_4 structures with $A = Py, Mp, Ep, Tr,$ and PEA for benchmark at the PBE+SOC level of theory.

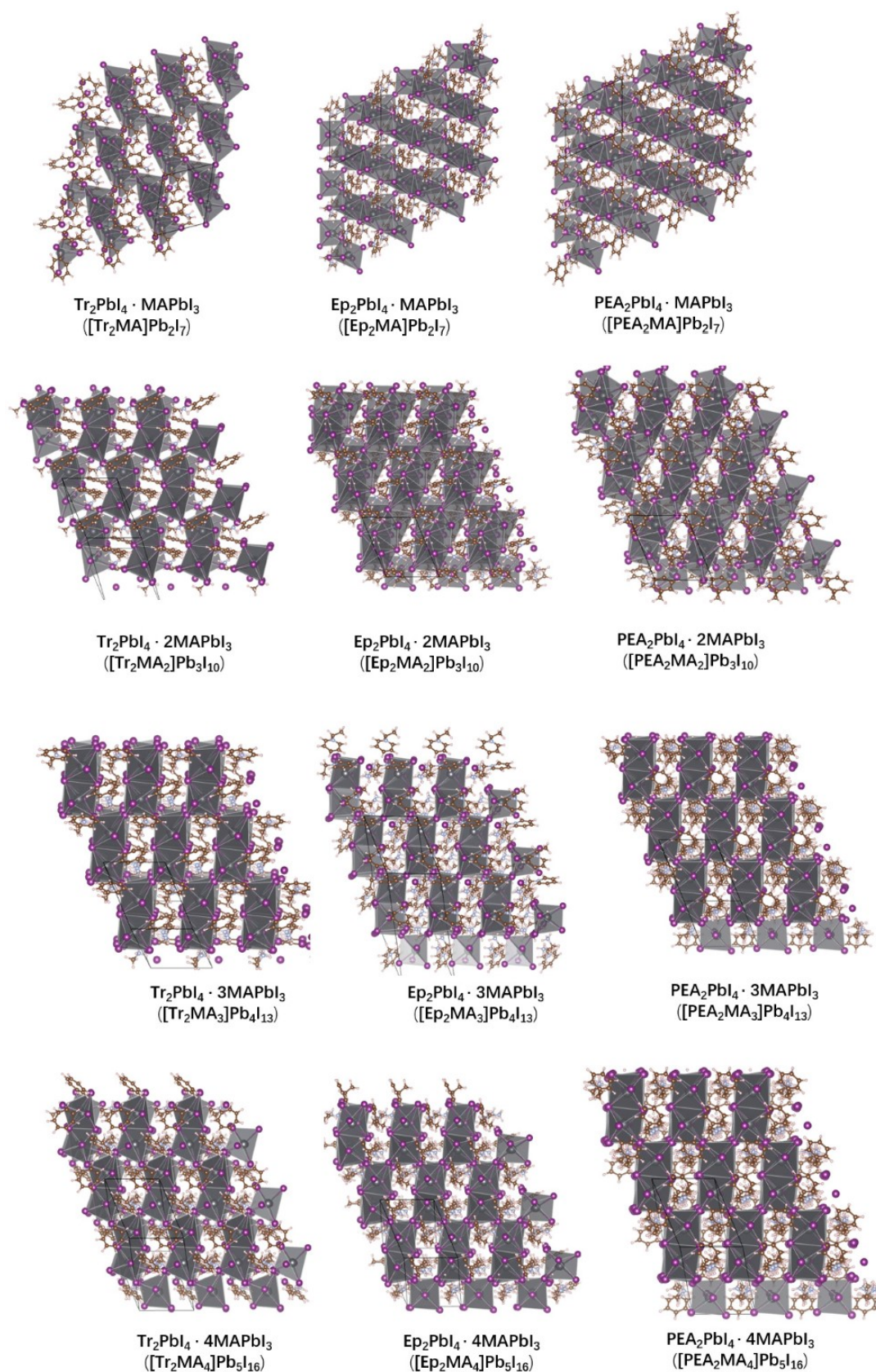


Figure S6: Optimized conformation (top view) of QLD perovskite structures $\text{A}_2\text{PbI}_4 \cdot n\text{MAPbI}_3$ $\text{A} = \text{Py}, \text{Mp}, \text{Ep}, \text{Tr}$ with $n = 1$ to 4.

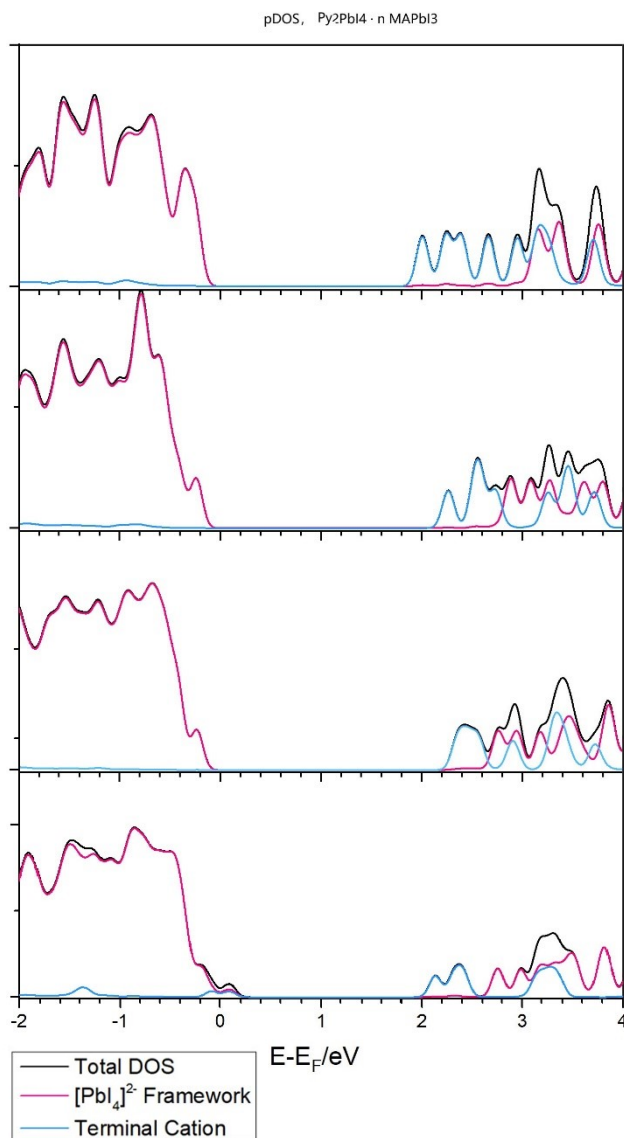


Figure S7: Computed density-of-states of QLD Py₂PbI₄ · nMAPbI₃ with $n = 1$ to 4 (top - bottom panels) at HS E06+SOC level of theory with an X_{CF} fraction being 0.38

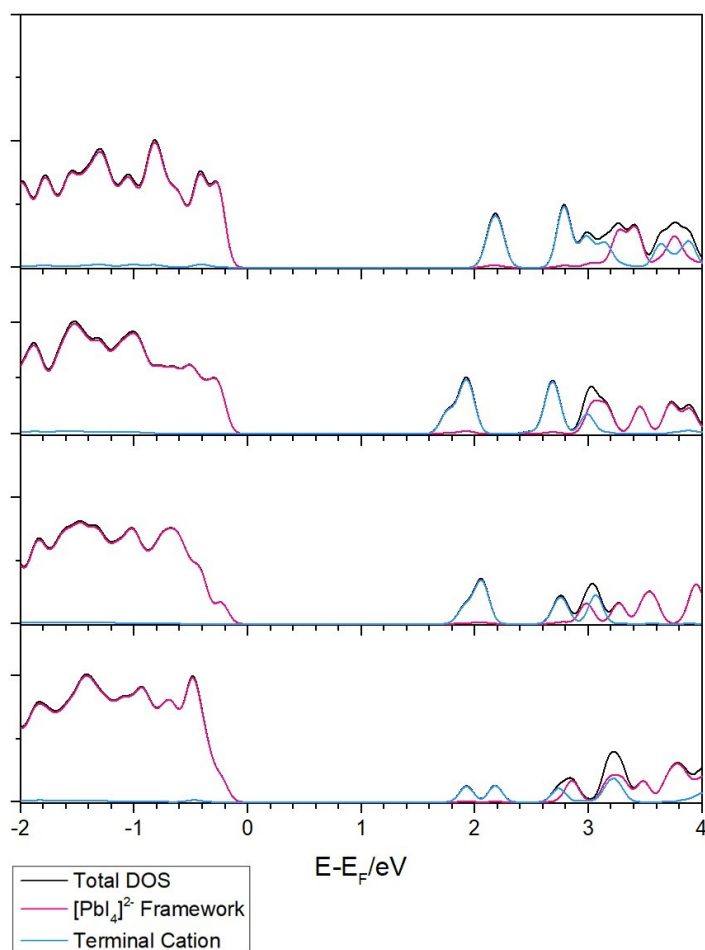


Figure S8: Computed density-of-states of QLD $\text{Mp}_2\text{Pbl}_4 \bullet n\text{MAPbl}_3$ with $n = 1$ to 4 (top - bottom panels) at HSE06+SOC level of theory with an XC_{HF} fraction being 0.38

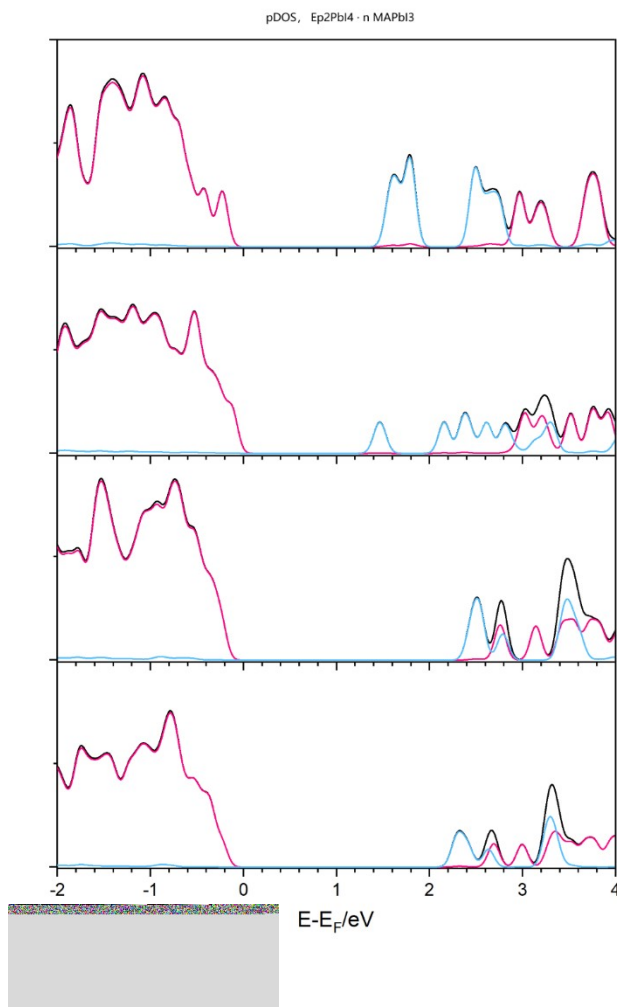


Figure S9: Computed density-of-states of QLD Ep₂PbI₄ · nMAPbI₃ with $n = 1$ to 4 (top - bottom panels) at HSE06+SOC level of theory with an XC_{HF} fraction being 0.38

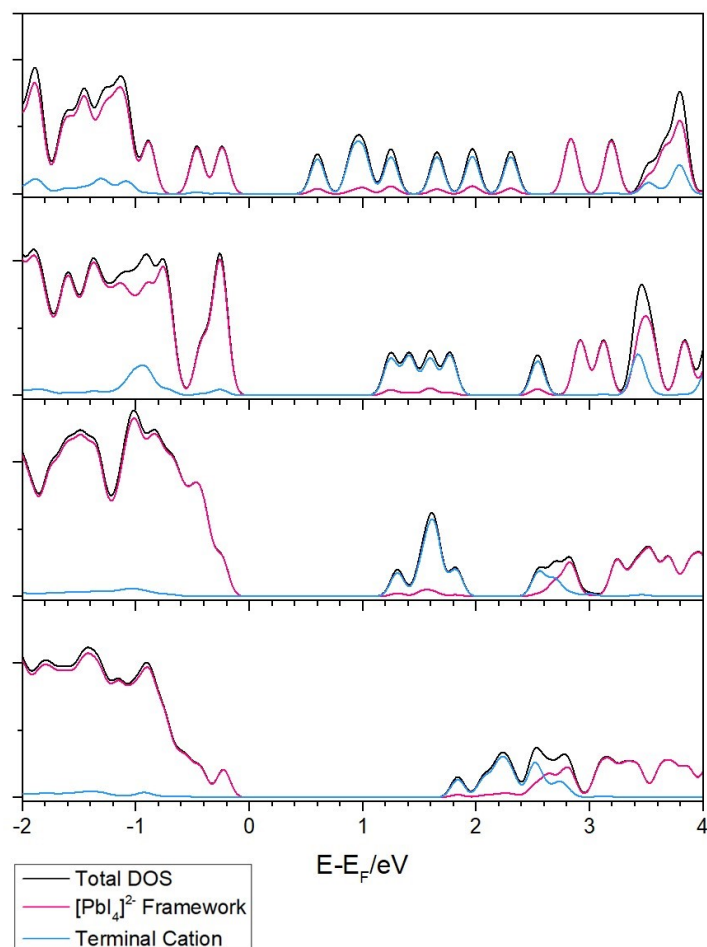


Figure S10: Computed density-of-states of QLD $\text{Tr}_2\text{PbI}_4 \bullet n\text{MAPbI}_3$ with $n = 1$ to 4 (top - bottom panels) at HSE06+SOC level of theory with an XC_{HF} fraction being 0.38.

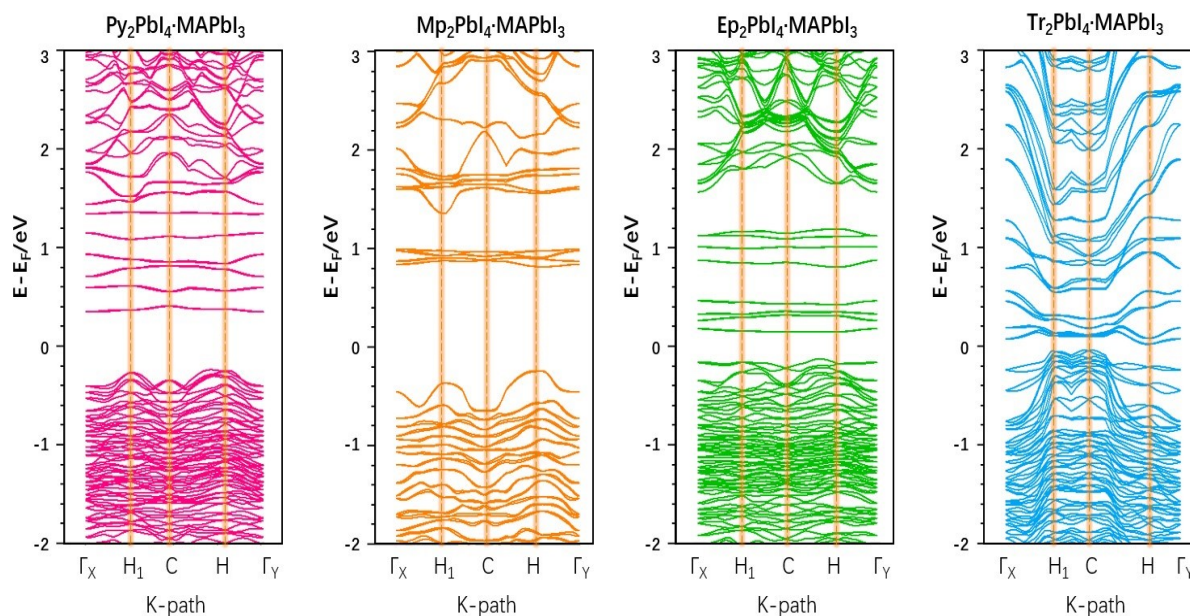


Figure S11: Computed band structure of QLD $\text{A}_2\text{PbI}_4 \bullet \text{MAPbI}_3$ ($n=1$) structures with $\text{A} = \text{Py}, \text{Mp}, \text{Ep}, \text{Tr}$ at PBE+SOC level of theory.

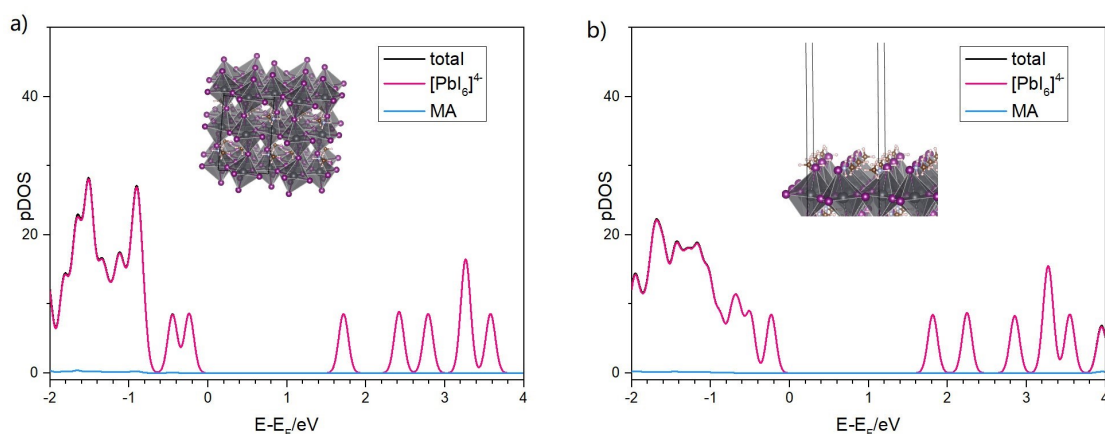


Figure S12: Computed projected density-of-state of MAPbI₃ with (a) bulk 3D structure and (b) QLD structure with 5 layers and a vacuum gap of 15 Å in the supercell.

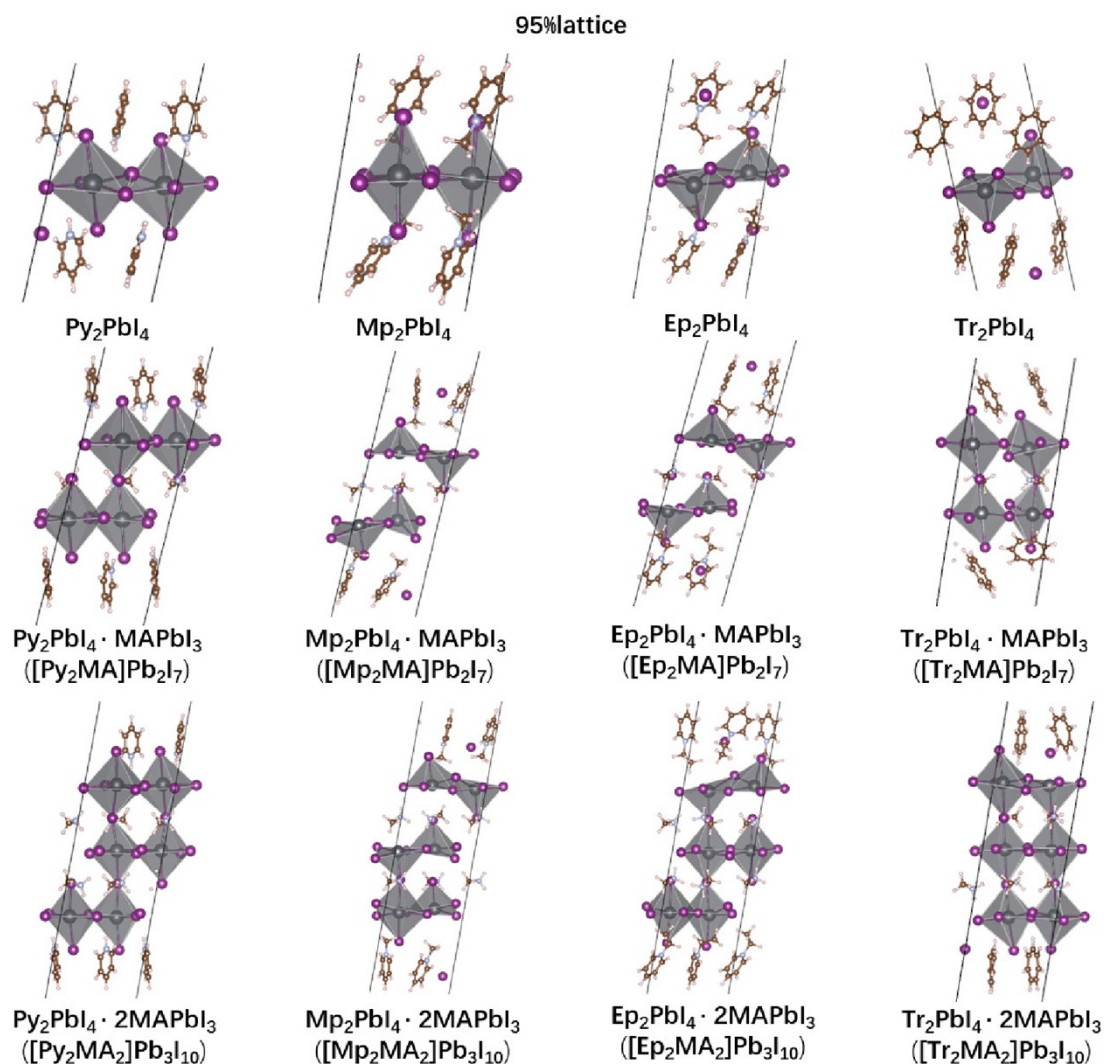


Figure S13: Optimized conformation (side view) of QLD perovskite structure A₂PbI₄ • nMAPbI₃ A = Py, Mp, Ep, Tr with n = 0 to 2 and with 95% lattice constant.

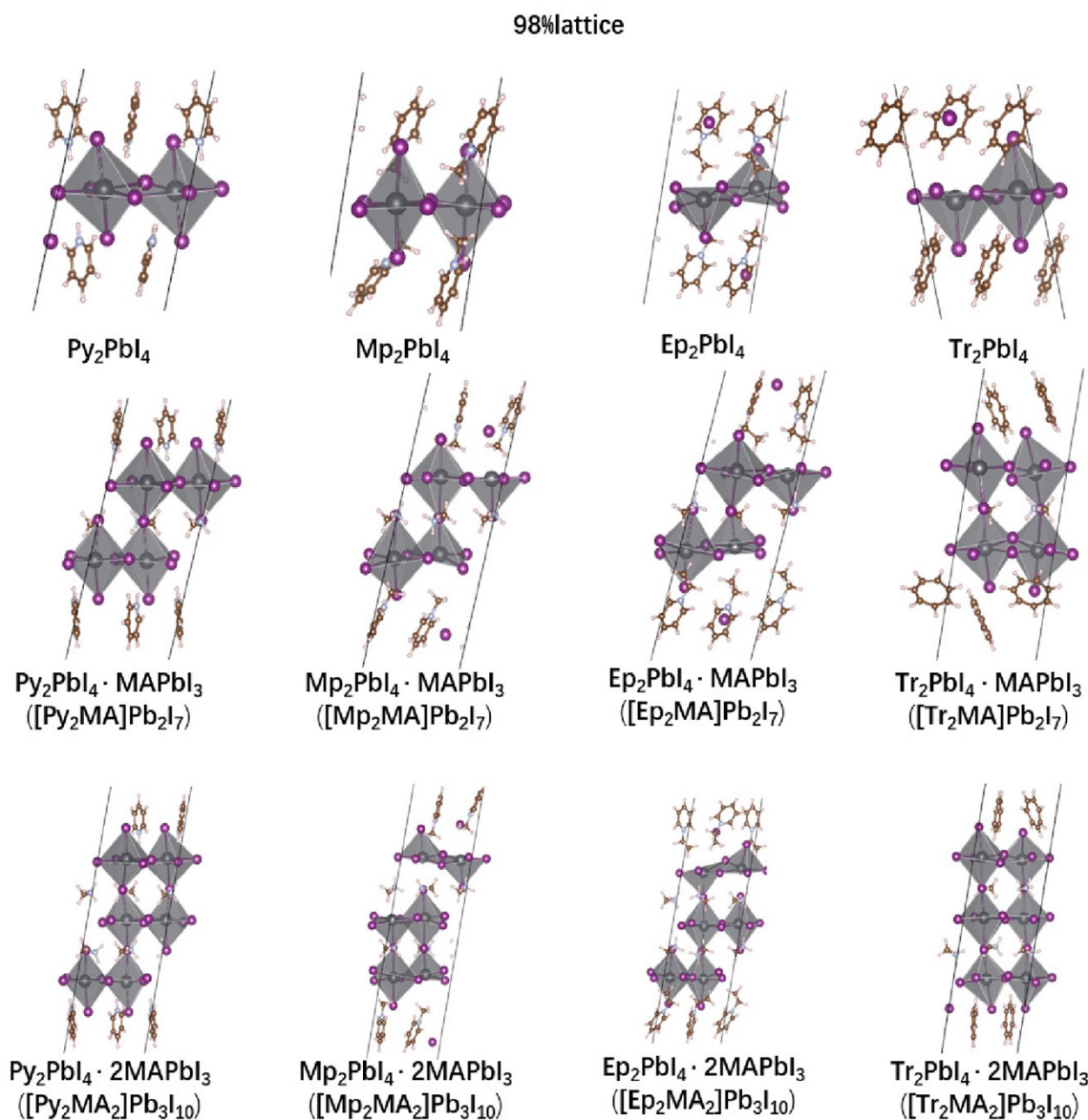


Figure S14: Optimized conformation (side view) of QLD perovskite structure $\text{A}_2\text{PbI}_4 \cdot n\text{MAPbI}_3$ $\text{A} = \text{Py}, \text{Mp}, \text{Ep}, \text{Tr}$ with $n = 0$ to 2 and with 98% lattice constant.

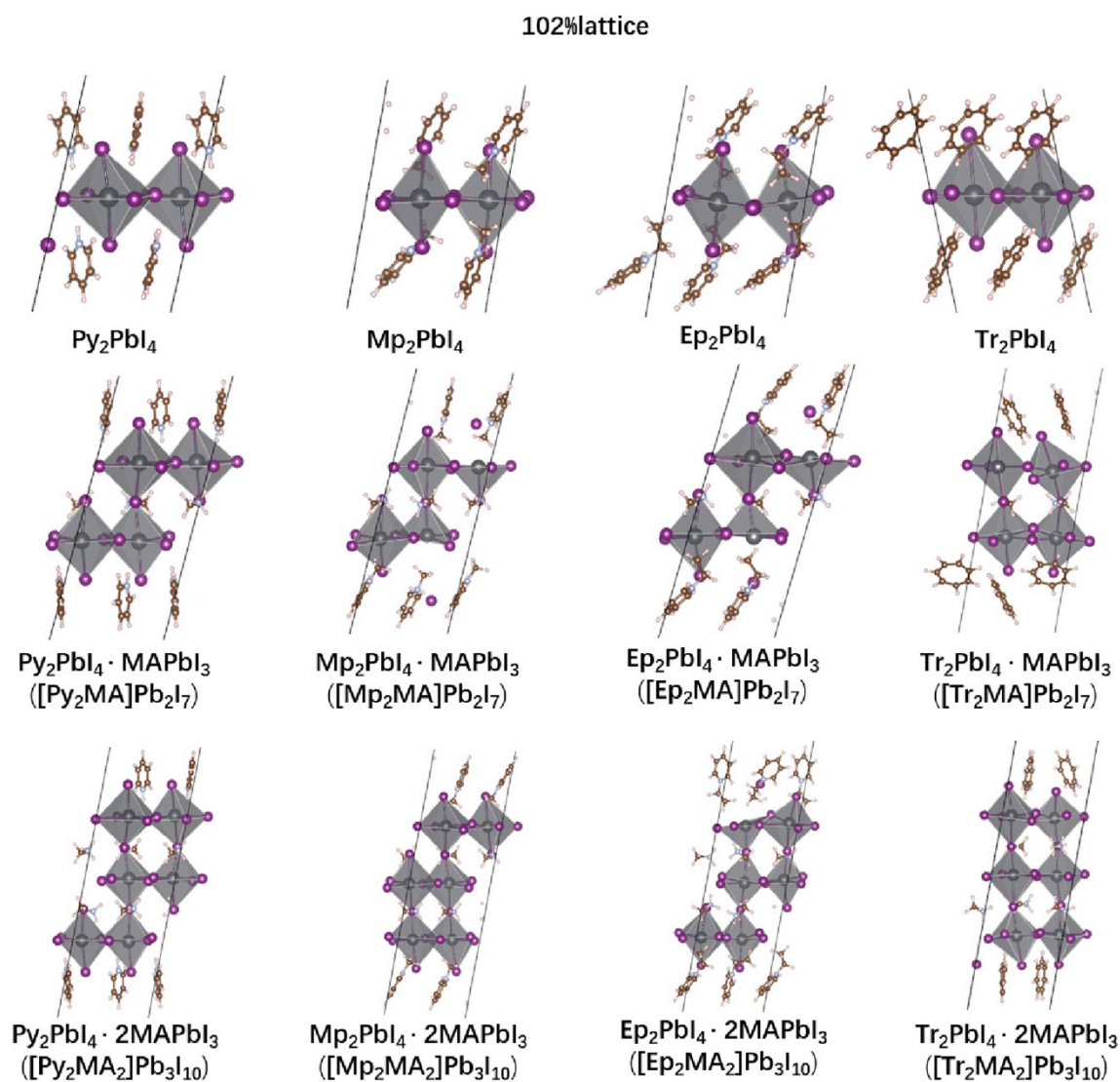


Figure S15: Optimized conformation (side view) of QLD perovskite structure $\text{A}_2\text{PbI}_4 \cdot n\text{MAPbI}_3$ $\text{A} = \text{Py}, \text{Mp}, \text{Ep}, \text{Tr}$ with $n = 0$ to 2 and with 102% lattice constant.

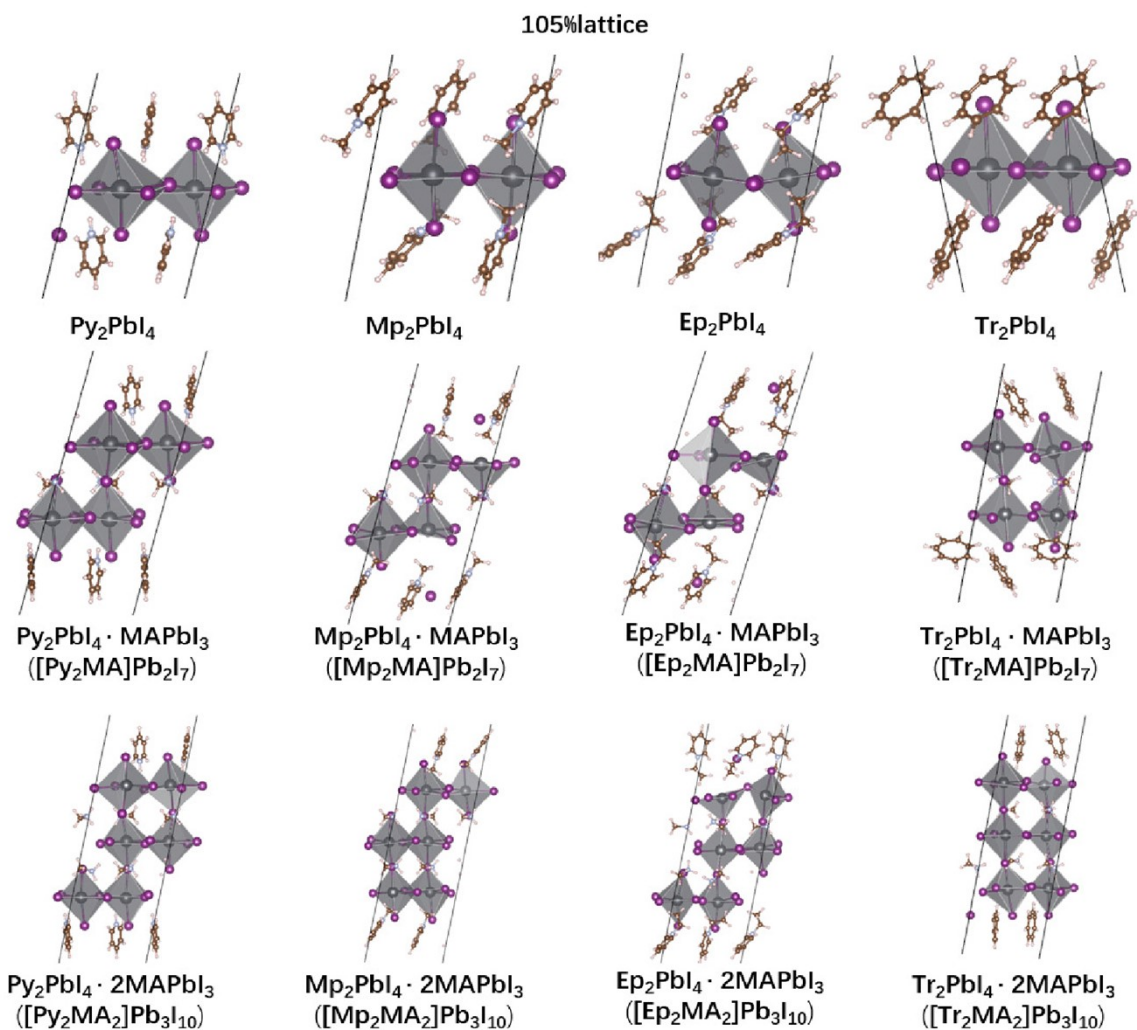


Figure S16: Optimized conformation (side view) of QLD perovskite structure $\text{A}_2\text{PbI}_4 \cdot n\text{MAPbI}_3$ $\text{A} = \text{Py}, \text{Mp}, \text{Ep}, \text{Tr}$ with $n = 0$ to 2 and with 105% lattice constant.

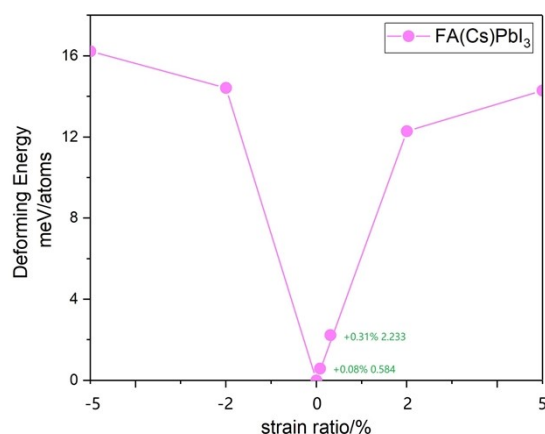


Figure S17: Computed deformation energy of $\text{FA}(\text{Cs})\text{PbI}_3$ adopted in *Science* (2025) **387**, 1069 at various strain ratios. The observed strain ratios in this article are marked out.

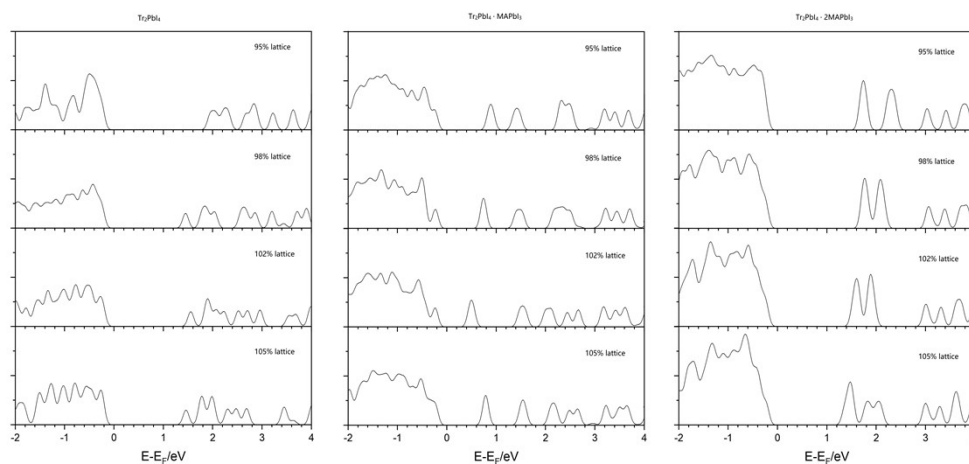


Figure S18: Computed density-of-state of $\text{Tr}_2\text{PbI}_4 \bullet n\text{MAPbI}_3$ with $n = 0$ to 2 and with various strain ratios.

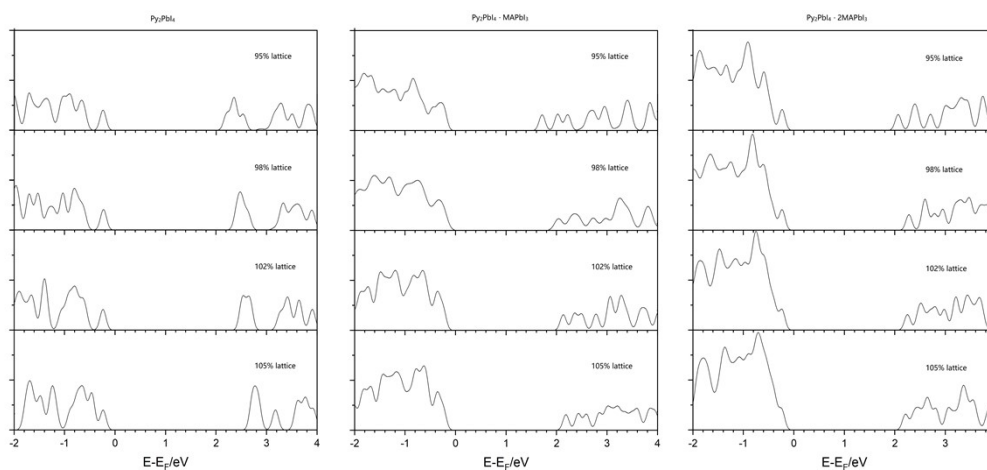


Figure S19: Computed density-of-state of $\text{Py}_2\text{PbI}_4 \bullet n\text{MAPbI}_3$ with $n = 0$ to 2 and with various strain ratios.

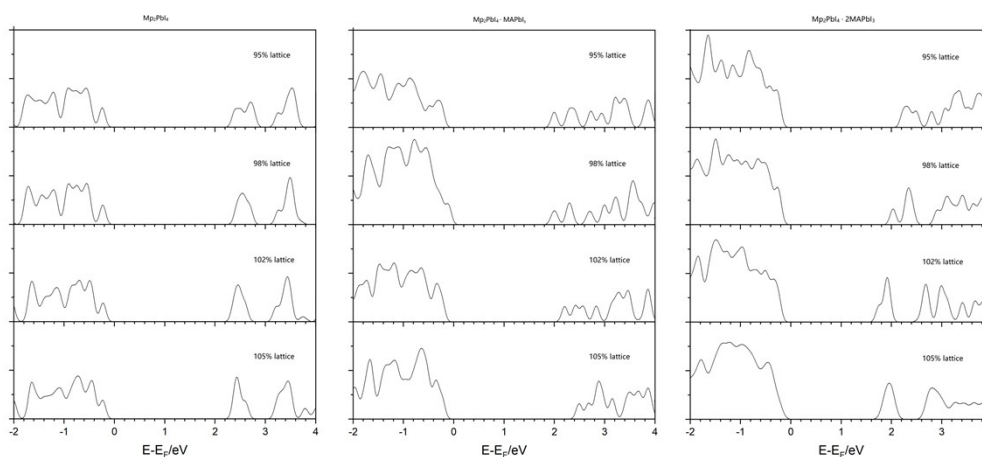


Figure S20: Computed density-of-state of $\text{Mp}_2\text{PbI}_4 \bullet n\text{MAPbI}_3$ with $n = 0$ to 2 and with various strain ratios.

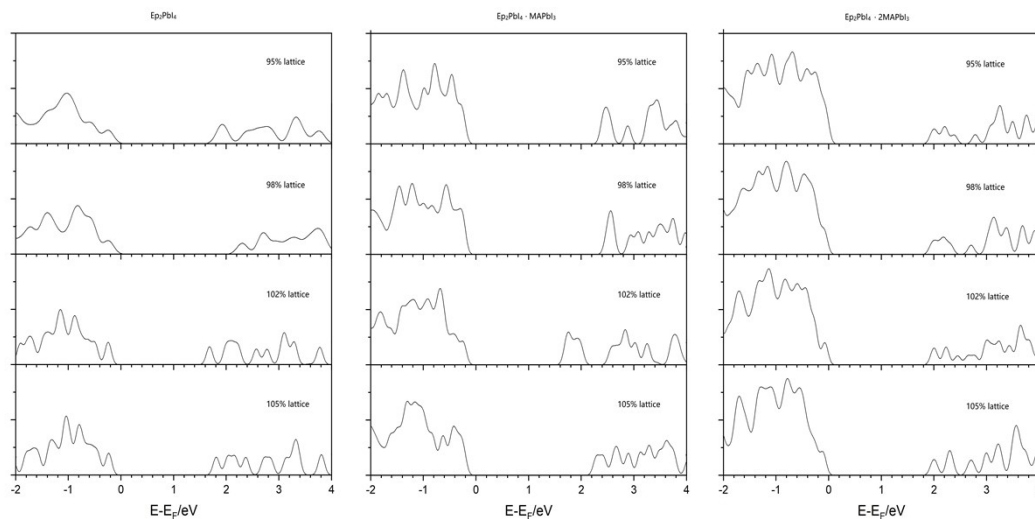


Figure S21: Computed density-of-state of $\text{Ep}_2\text{PbI}_4 \cdot n\text{MAPbI}_3$ with $n = 0$ to 2 and with various strain ratios.

Table S1: Calculated geometric data of the optimized conformations of QLD CPAC perovskite $\text{A}_2\text{PbI}_4 \cdot n \text{MAPbI}_3$ structures with $n = 1$ to 4

Spacer Category		Py	Mp	Ep	Tr
Max $d_{\text{Pb-I}}/\text{\AA}$	n=1	3.45	4.14	3.76	3.62
	n=2	3.59	3.57	5.06	3.59
	n=3	3.31	3.46	6.20	3.84
	n=4	3.34	4.91	6.53	4.60
Average $d_{\text{Pb-I}}/\text{\AA}$	n=1	3.30	3.28	3.31	3.29
	n=2	3.33	3.28	3.39	3.28
	n=3	3.25	3.29	3.21	3.24
	n=4	3.26	3.32	3.23	3.32
$\angle\text{I-Pb-I}/\text{deg.}$	n=1	97.1	98.6	98.7	100.8
	n=2	98.6	96.48	116.34	116.63
	n=3	96.27	92.78	105.32	100.90
	n=4	100.17	106.71	111.79	101.96
$d_{\text{A-I}}/\text{\AA}$	n=1	3.54(2.86)	3.79	4.05	3.70(2.85)
	n=2	3.57(2.58)	3.36	3.78	3.69(2.85)
	n=3	3.43(2.39)	4.44	3.98	3.88(2.73)
	n=4	3.71(2.58)	4.28	3.99	3.90(2.82)
$h/\text{\AA}$	n=1	18.47	21.33	20.46	21.13
	n=2	24.16	26.79	27.21	26.75
	n=3	30.08	32.44	34.41	34.21
	n=4	38.73	40.24	40.37	39.76

Table S2: Calculated free energies (in eV) of the optimized conformations of QLD PAC perovskite $A_2PbI_4 \bullet n MAPbI_3$ structures with $n = 1$ to 4

Spacer Category	Py	Mp	Ep	Tr
$n = 1$	-429.18	-494.74	-562.90	-481.22
$n = 2$	-531.75	-596.84	-664.76	-580.14
$n = 3$	-635.06	-700.86	-767.65	-680.97
$n = 4$	-738.59	-810.18	-870.13	-786.71

Table S3: Calculated formation energies (in meV/atoms) of the optimized conformations of QLD PAC perovskite $A_2PbI_4 \bullet n MAPbI_3$ structures with $n = 1$ to 4

E_{form} follows the procession of $2AI + nMAI + (n+1)PbI_2 \rightarrow A_2PbI_4 \bullet n MAPbI_3$

Spacer Category	Py	Mp	Ep	Tr
$n = 1$	-96.2975	-70.8127	-134.9811	-60.0866
$n = 2$	-89.4830	-86.6542	-123.5330	-85.8491
$n = 3$	-125.5692	-108.9014	-123.4488	-87.1335
$n = 4$	-121.7064	-158.9325	-171.2101	-118.3771

Table S4: Calculated phase-segregation energies (in meV/atoms) of the optimized conformations of QLD PAC perovskite $A_2PbI_4 \bullet n MAPbI_3$ structures with $n = 1$ to 4

E_{seg} follows the procession of $A_2PbI_4 \bullet n MAPbI_3 \rightarrow A_2PbI_4 + (MAPbI_3)_n$

Spacer Category	Py	Mp	Ep	Tr
$n = 1$	107.61638	10.53029	42.01524	58.81978
$n = 2$	91.77215	27.32841	52.62792	77.29956
$n = 3$	77.48840	23.14085	51.42889	88.77147
$n = 4$	74.69879	19.63120	53.18080	84.03623

Table S5: Calculated layer-segregation energies (in meV/atoms) of the optimized conformations of QLD PAC perovskite $A_2PbI_4 \cdot n MAPbI_3$ structures with $n = 1$ to 4 E_{seg} follows the procession of $A_2PbI_4 \cdot n MAPbI_3 \rightarrow A_2PbI_4 \cdot (n-1) MAPbI_3 + MAPbI_3$

Spacer Category	Py	Mp	Ep	Tr
$n = 1$	107.61638	10.53029	42.01524	58.81978
$n = 2$	17.30024	20.20840	20.12557	56.30756
$n = 3$	6.49481	0.30483	8.51692	27.72553
$n = 4$	3.51592	37.46852	9.76681	12.69667

Table S6: Calculated deformation energies (in meV/atoms) of the optimized conformations of QLD PAC perovskite $A_2PbI_4 \cdot n MAPbI_3$ structures with $n = 0$ to 2 and with various strain ratios $E_{dist.}$ follows the procession of $A_2PbI_4 \cdot n MAPbI_3 pris. \rightarrow A_2PbI_4 \cdot n MAPbI_3 str.$

thickness	strain ratio	Py	Mp	Ep	Tr
$n=0$	-5%	106.67	5.25	7.13	72.85
	-2%	68.73	1.14	0.45	62.31
	+2%	48.49	0.35	8.36	48.40
	+5%	39.38	17.17	6.11	39.47
$n=1$	-5%	53.88	27.53	36.16	28.55
	-2%	24.27	19.75	29.56	20.71
	+2%	14.88	14.67	33.50	16.40
	+5%	12.22	13.07	24.38	13.59
$n=2$	-5%	68.56	34.91	22.93	52.95
	-2%	32.27	24.03	14.62	31.61
	+2%	21.65	20.93	14.53	22.38
	+5%	21.85	13.25	13.89	20.22

Table S7: Calculated maximum surface Pb-I distance (in Å) of the optimized conformations of QLD PAC perovskite $A_2PbI_4 \cdot n$ MAPbI₃ structures with $n = 0$ to 2 and with various strain ratios

thickness	strain ratio	Py	Mp	Ep	Tr
n=0	-5%	3.37	3.59	7.27	7.39
	-2%	3.35	3.48	6.39	5.31
	+2%	3.34	3.48	3.59	3.92
	+5%	3.46	3.51	3.56	3.73
n=1	-5%	3.30	6.70	8.08	3.63
	-2%	3.38	4.17	7.90	3.54
	+2%	3.52	4.17	3.91	3.63
	+5%	3.60	4.48	6.72	3.60
n=2	-5%	3.41	4.89	5.60	3.88
	-2%	3.51	4.33	5.31	3.58
	+2%	3.66	3.47	5.05	3.61
	+5%	3.56	3.61	5.18	3.67

Table S8: Calculated band gaps (in eV) of the optimized conformations of QLD PAC perovskite $A_2PbI_4 \cdot n$ MAPbI₃ structures with $n = 0$ to 2 and with various strain ratios

At HSE06+SOC level of theory with an XC_{HF} fraction of 0.38

thickness	strain ratio	Py	Mp	Ep	Tr
n=0	-5%	1.99	2.17	1.66	1.21
	-2%	2.19	2.26	1.92	1.23
	+2%	2.52	2.37	1.56	1.78
	+5%	2.54	2.43	1.51	1.69
n=1	-5%	1.50	1.78	2.24	0.62
	-2%	1.76	1.84	2.28	0.65
	+2%	2.01	2.16	1.50	0.91
	+5%	2.04	2.27	2.07	1.00
n=2	-5%	1.85	2.02	2.00	1.47
	-2%	2.06	1.85	1.78	1.50
	+2%	2.08	1.53	1.45	1.36
	+5%	1.99	1.58	1.53	1.59